IEEE Access
Multidisciplinary | Rapid Review | Open Access Journal

Received June 6, 2019, accepted June 17, 2019, date of publication June 24, 2019, date of current version July 11, 2019.

Digital Object Identifier 10.1109/ACCESS.2019.2924391

Printed Circuit Board Implementation of Wideband Radial Power Combiner

SAYYED-HOSSEIN JAVID-HOSSEINI AND VAHID NAYYERI, (Senior Member, IEEE)
School of New Technologies and Antenna and Microwave Research Laboratory, Iran University of Science and Technology, Tehran 1684613114, Iran
Corresponding author: Vahid Nayyeri (nayyeri@iust.ac.ir)

ABSTRACT This paper presents a new approach to design and implementation of a wideband microstrip radial power combiner with a planar structure in a way that it can be simply and inexpensively fabricated using a standard multilayer printed circuit board (PCB) technology. A 14-way power combiner with a two-octave bandwidth (1.5–6 GHz) is designed and fabricated on a three-layer PCB. Our measurements showed an amplitude and phase balance of ±0.75 dB and ±4.5 degrees, respectively, between the input ports. The main (output) port exhibited a reflection lower than −10 dB.

INDEX TERMS Distributed computing, manufacturing process, microstrip, multilayer circuit board, multi-physics simulation, N-way power combiner, planar circuits, power handling, power splitter, printed circuit board, radial power combiner, wideband.

I. INTRODUCTION

The need for RF and microwave power in communications and military systems have usually been and still is greater than what a single solid-state device can provide. One can overcome this by combining the output power of multiple solid-state transistors with each other. Many different power combining methods have been investigated through the years and a comprehensive introduction of these methods can be found in the literature [1]–[4]. Corporate combining method is a good choice for combining the power of a small number of devices, but they will cause a considerable amount of loss as the number of combined devices increases since the total length of lossy transmission lines goes up quickly with the number of devices combined [5]. Besides that, using corporate method for combining a large number of devices introduces a high level of phase and amplitude unbalances which reduces the combining performance. On the other hand, another approach, namely N-way power combining, in which the input devices are combined in one step, has advantages over the corporate technique when the number of devices is high. These advantages include a lower insertion loss and also a better phase and amplitude balance. As the main drawback, N-way power combiners typically suffer from lack of good isolation between the input ports; however, once the number of combined devices gets large enough they provide acceptable isolation between the peripheral ports [6].

The associate editor coordinating the review of this manuscript and approving it for publication was Feng Lin.

Radial combiners [7]–[9] are an important class of N-way combiners. Due to their inherent symmetry, the amplitude and phase of their input ports are well balanced. Radial combiners are usually implemented using waveguides [10]–[12] or microstrip transmission lines [5], [13]–[15]. By comparing them, waveguide radial power combiners typically have a lower loss, which is an inherent advantage of waveguides over microstrip lines. On the other hand, microstrip radial power combiners can provide a wider bandwidth.

A drawback of radial power combiners is that they are complicated to manufacture. Specifically speaking, the ones based on waveguide require precise machine work, which is both time-consuming and expensive. Microstrip radial power combiners are much easier to manufacture; however, they require the output port to be vertically attached to the center of the combiner very precisely (in order to prevent the propagation of higher order modes) [5], [14], which in turn causes manufacturing difficulties. in addition, it does not help that the impedance of this central (output) port is usually much less than 50 Ω; hence, in a wideband microstrip radial power combiner, the central port is not just a simple connector, rather a machined coaxial line with a step or taper profile which gradually increases the impedance of the port to 50 Ω [5], [14], [15]. This machining process which is required to be performed with high accuracy to preserve the phase and amplitude balance of the power combiner also increases the cost and time of manufacturing.

In this paper, we introduce a new design approach for wideband microstrip radial power combiner to simplify the

 This work is licensed under a Creative Commons Attribution 3.0 License. For more information, see http://creativecommons.org/licenses/by/3.0/

manufacturing process. In the proposed method, the combiner is designed in a way that it is fabricated simply using a standard multilayer printed circuit board (PCB) technology without the need for any machine work, thereby, cutting the cost and manufacturing time of the product significantly. Such an approach eliminating machine work, to the best of the authors' knowledge, has not been previously reported in the literature. The proposed method is applied to design and fabricate a fully planar wideband microstrip radial power combiner on a three-layer PCB.

In section II, the design procedure is discussed and the proposed structure is described. The simulation and optimization processes are explained and the section ends with a discussion about the power handling of the proposed design. In section III, simulation and measurement results are presented. A comparison between the present work and some state-of-the-art radial power combiners is also made in this section. The paper ends with section IV where a conclusion is made.

II. STRUCTURE AND DESIGN

Figure 1a shows the schematic of the proposed design and Figure 1b shows the exploded view of the proposed combiner, using a three-layer PCB consisting of two Rogers RO4003 substrates (having a dielectric constant of 3.55 and a loss tangent of 0.0021-0.0027) with a thicknesses of 1.5 mm and 0.5 mm. The input and output sections of the combiner are printed on the top and bottom metallization layers and are connected to each other by a via at the center of the board. The middle metallization layer is a mutual ground in between them. To provide a better understanding of the structure, it is explained in details in the following.

A. INPUT SECTION

As shown in Figure 2a, the input section of the combiner consists of 14 identical peripheral ports, each of which is connected to the center of the combiner by a tapered microstrip transmission line. Each taper is designed in a way that the characteristic impedance of the line changes by a linear profile from 50 Ω (i.e., W1 = 3.37 mm) at the perimeter where the input ports are located, to 100 Ω (i.e., W2 = 0.83 mm) at the center where all 14 tapers meet each other on the periphery of a central disk. The length of the tapers (L1) was set to be long enough to provide a good matching (i.e., a return loss of 20 dB) between 50 Ω and 100 Ω at the lowest frequency of interest, i.e., 1.5 GHz. In fact, having a good impedance conversion from 50 Ω to 100 Ω is the main dictating factor for the radius of the combiner. Notice that, the reason for using a taper is to increase the impedance at the central disk, where all 14 tapers meet. Specifically speaking, by using a tapered line and increasing the impedance from 50 Ω to 100 Ω, instead of working with an impedance of $50/14 = 3.57$ Ω at the center where all 14 lines meet (which is a very hard impedance to work with) we are dealing with an impedance of $100/14 = 7.14$ Ω; still not perfect but much better than 3.57 Ω. While it would make things even easier

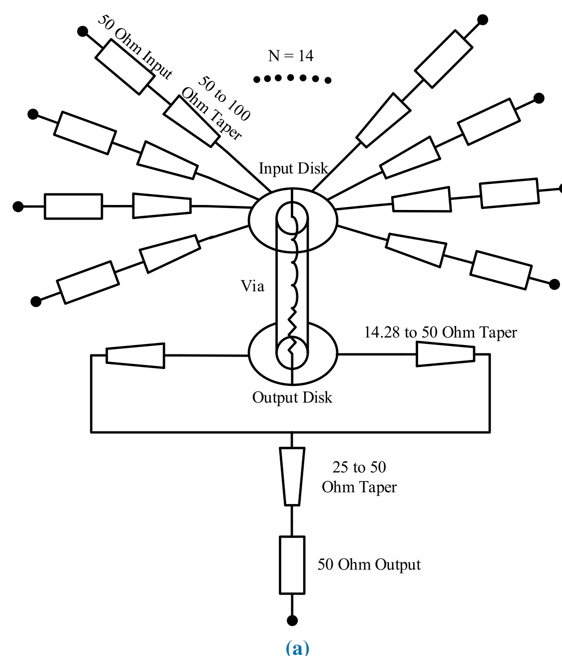

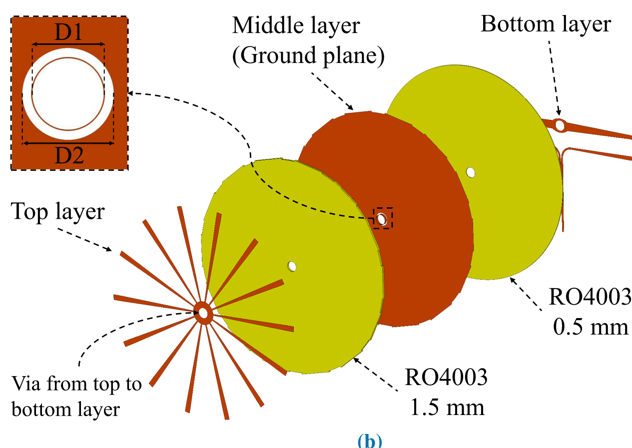

FIGURE 1. The proposed radial combiner: (a) A schematic of the design showing 14 input ports connecting to a via in the center. The via takes the signal to the other side of the board and delivers it to the output port using matching tapers and transmission lines. (b) The exploded view of the proposed combiner, designed on a 3-layer PCB.

to further increase the impedance of the tapers at the center (and consequently the total impedance at the central point), doing so will result in very long tapers (and hence, a large size of combiner) and also very thin lines having a negative impact on power handling.

As seen in Figure 2a, all 14 tapered lines meet each other at the periphery of a circular disk with a diameter of D3 on the input side of the combiner. The ground plane and this central disk, which in microstrip radial power combiners is usually called a launcher, form a parallel plate radial waveguide [5]. The diameter of the disk determines propagating modes in the waveguide and so must be chosen carefully to prevent propagation of high order modes. Unlike the fundamental mode, whose electric field is constant in the ϕ direction, that of the higher order modes changes with ϕ and will cause a significant phase unbalance (between the input ports) if they

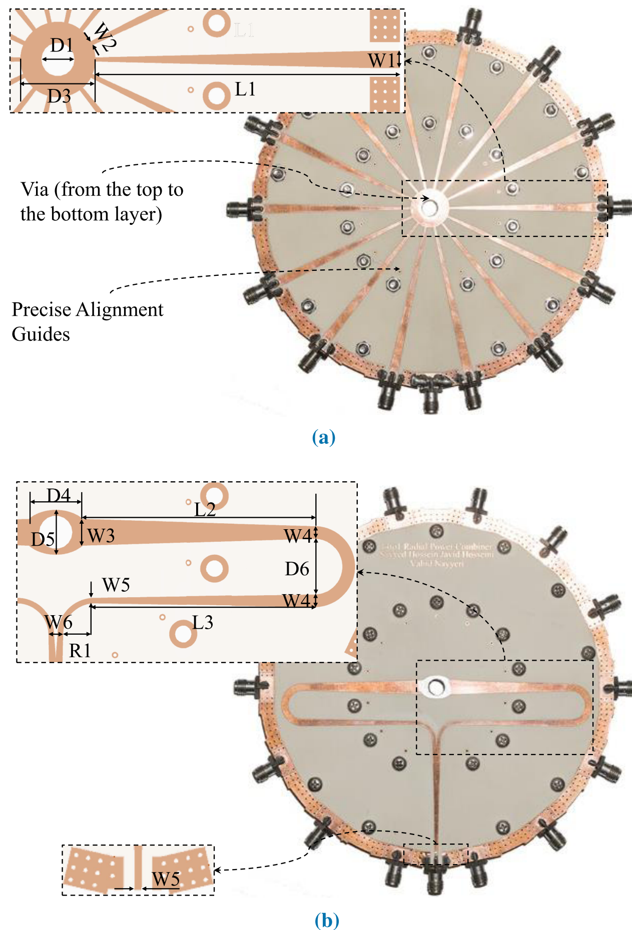

FIGURE 2. Fabricated combiner: (a) top and (b) bottom layers of metalization.

are not cared for. The diameter of this disk (D3 in Figure 2a) was set as an optimization parameter and obtained through an optimization procedure which will be discussed in detail in subsection II-D.

B. TRANSMISSION BETWEEN INPUT AND OUTPUT SECTIONS

As seen in Figure 1a, the input launcher (disk) is connected to the bottom layer - the output side - with a via. This via passes through the ground plane, which lays between the top and the bottom layers but has no connection with it. The via diameter and the spacing between the via and the ground plane which are visible in the magnified section of Figure 1b are two design parameters which need to be determined.

A via in general has some inductance. This inductance is inversely proportional to the via diameter and directly proportional to frequency. The diameter of the via (D1) should be large enough that its inductance becomes negligible at the highest frequency of interest, but not so large to have a negative impact on the phase and amplitude balances. Using the via model in the Advanced Design System (ADS), the via diameter was set to a minimum value which results in a negligible inductance at the highest frequency of interest, i.e., 6 GHz.

TABLE 1. Value of design parameters indicated in Figure 1b, Figure 2a and Figure 2b.

Parameter	Value	Unit	Parameter	Value	Unit
W1	3.51	mm	L3	45.1	mm
W2	0.84	mm	D1	6.82	mm
W3	5.5	mm	D2	8.64	mm
W4	2.56	mm	D3	14.34	mm
W5	1.16	mm	D4	10.96	mm
W6	2.97	mm	D5	9.16	mm
L1	62.34	mm	D6	11.42	mm
L2	47.53	mm	R1	6.43	mm

On the other hand, the set of the central via and the ground plane can be approximately modeled by a coaxial transmission line with a core diameter of D1 (via diameter) and an outer diameter of D2. The equation for the characteristic impedance of a coaxial line was used to obtain D2 (and consequently the spacing between via and the ground plane). Having the via diameter (D1) and assuming that the characteristic impedance of this coaxial line is matched to that at the center of the input section i.e., $100/14 = 7.14\ \Omega$, D2 was calculated.

C. OUTPUT SECTION

On the output side, as shown in Figure 2b, the via ends at a central ellipse which plays the role of the launcher in this side. Observation of the electric field distribution (obtained by full-wave simulations using CST microwave studio [16]) revealed that using a circular disk as launcher leads to a considerable amplitude unbalance between the input ports. However, by changing the circular disk into an ellipse and optimizing both its major (D4) and minor (D5) axes we could retain the amplitude balance.

Essentially, the task of the output section is to deliver the signal which was received from the via to a 50 Ω output port. This may first seem like a simple task but the significant impedance difference between the via and the output port and also very wide bandwidth make it more complicated. As mentioned earlier, the impedance of the central via is 7.14 Ω. Having a simple taper between this via and a 50 Ω output port is not possible since a 7.14 Ω microstrip line is too wide - almost twice the via diameter - and so cannot be effectively connected to the via. To address this problem, as shown in Figure 2b, two parallel lines were used to take the signal from the via to the output port. Since the lines are in parallel, each should have a characteristic impedance of $7.14 \times 2 = 14.28\ \Omega$. As seen in Figure 2b, a 14.28 Ω line has a width of not much different from the via diameter and so can be easily connected to the central via. From this point, each line is gradually and with a linear profile tapered to an impedance of 50 Ω, where they are joined together and form a 25 Ω line. Finally using another linear tapered line,

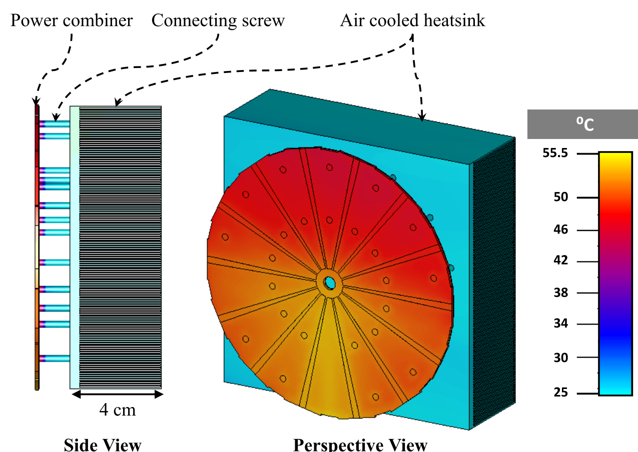

FIGURE 3. The temperature distribution when the input power (as a splitter) is 100 W RMS and the combiner is mounted on an air cooled heatsink which is actively cooled using two fans.

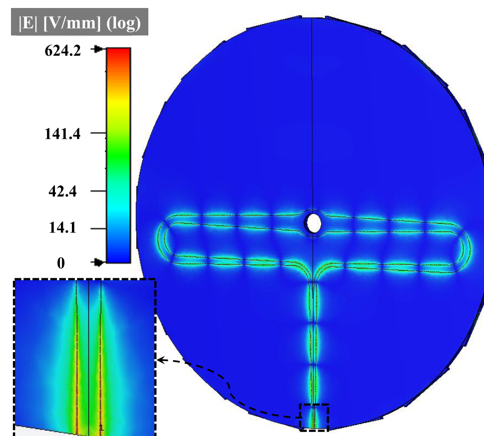

FIGURE 4. Electric field intensity distribution on the board for 100 W RMS of input power (as a splitter).

this impedance was transformed to 50 Ω at the perimeter of the combiner where the output port is placed. It should be noted that the lengths of the tapered lines were set such that they provide a good matching from 1.5 GHz.

D. OPTIMIZATION PROCEDURE

Once the width and length of the tapered lines, the via diameter, and also the spacing between the via and the ground plane was obtained in the aforementioned method, the diameters of the central disk on the top layer (D3) and the major and minor axes of the central ellipse on the bottom layer (D4 and D5) were determined in an optimization procedure. A full-wave optimization was carried out in CST microwave studio. Trust Region Framework algorithm with a semi-global setting was used to find the optimum values of these three parameters. The optimization goals were set to achieve a phase and an amplitude balance of better than $\pm 2.5°$ and ± 0.5 dB, respectively. Having a return loss better than -15 dB at the output port in the frequency band of 1.5 GHz to 6 GHz was set as the third goal.

Once the optimization converged, all the design parameters were slightly tuned for a better performance of the combiner in the bandwidth of 1.5 to 6 GHz. For this purpose, Trust Region Framework of CST microwave studio with a local setting (which is a local optimization algorithm) was used. The obtained optimum values are given in TABLE 1.

It should be noted that the frequency solver of CST was used for full-wave simulations because tetrahedral meshes of this solver are better matched to the geometry of the structure which is mostly comprised of curves and lines that are not aligned with Cartesian axes. However, for such a wideband problem, the frequency solver needs to solve the problem in many frequency samples, a task which results in a very long optimization time. CST's distributed computing capability was used to solve this problem. By using this approach, simulations at different frequency samples are distributed between different machines; hence significantly reducing the optimization time.

E. POWER HANDLING CONSIDERATIONS

The power handling of the combiner was investigated from two different aspects. The heat sinking capability of the combiner and the maximum electrical field that it can handle before a breakdown happens. For the heat sinking problem, coupled electromagnetic-thermal simulations where performed in CST. In this simulation technique, the high frequency solver of CST's microwave studio calculates the electric (and magnetic) loss in the structure. The results are then handed over to the CST MPHYSICS (multi-physics) studio [16] where it forms the losses into a heat source. This heat source can then be scaled to match any arbitrary input power since the relation between the losses and the input power is linear.

In our simulation, the combiner was assumed to be mounted on a finned heatsink with a thickness of 4 cm which is cooled using two standard $2.5 \times 4 \times 4$ cm fans with a combined volume flew rate of 63.6 CFM. Notice that using actively air-cooled heatsinks is very common in high power systems. The ambient temperature was set to 25°C. Figure 3 shows the resultant temperature distribution for an input power (as a splitter) of 100 W RMS. At the hottest area of the board (which is around the combine port), the temperature reaches 55.5°C which is quite acceptable for a PCB. Furthermore, the heat-handling of the design was also investigated under two other conditions: 1) the combiner is mounted on a passively air cooled heatsink (the same heatsink but without fans) and 2) it is not mounted on a heatsink (as a free stand board). Assuming the same input power (100 W RMS), the results of our coupled electromagnetic-thermal simulations showed that at the hottest area, the temperature reaches to 68°C and 147°C, respectively, which are in the safe operating range of the used substrate (RO400C) according to its datasheet [25]. It should be noted that in these simulations, the source was assumed to be continues-wave. In the case of a pulsed RF source, the steady state temperatures are sure to be lower depending on the duty cycle of the pulse.

For the electric field breakdown consideration, similar to [17], [18], simulations were carried out in CST studio to

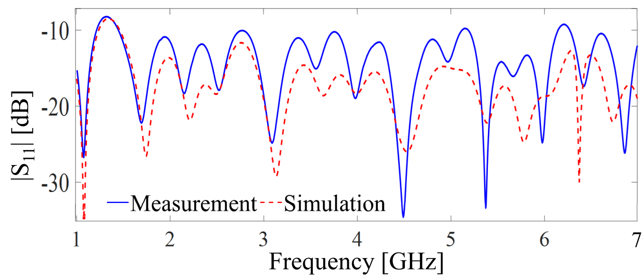

FIGURE 5. The simulated and measured return loss of the output (combine) port.

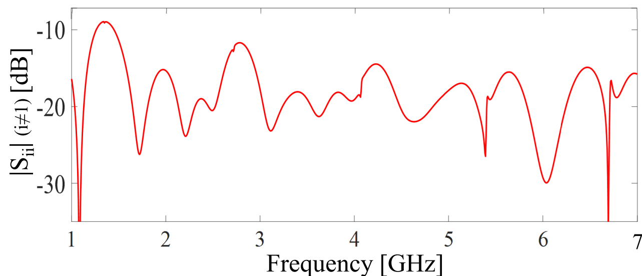

FIGURE 6. Simulation of the return loss of the input (split) ports in even mode of operation.

evaluate the maximum electric field on the board. Assuming an input power (as a splitter) of 100 W RMS, as shown in Figure 4, the maximum electric field is 624.2 V/mm and this maximum is concentrated around the edges of the input (as a splitter) 50 Ohm transmission line, which is enlarged in the inset of Figure 4. On the other hand, according to the data provided by the Rogers company [25], the used substrate (RO4003C) can withstands an electric field intensity of 31.2 kV/mm. According to these numbers, even with an input power of 100 W RMS, we are still far away from the breakdown point of the substrate. The above analyses demonstrate that for the designed power combiner, the electric field breakdown is not a concern, but it is better to address the heat-handling with an active or passive heatsink.

III. RESULTS AND DISCUSSION

The designed radial power combiner was fabricated using PCB technology and 15 high-frequency SMA connectors were mounted on the board as shown in Figure 2a and Figure 2b. In the test, the fabricated combiner was tested using a two-port vector network analyzer, while the ports not under test were terminated by matched loads.

The measured return loss of the output port is shown in Figure 5 wherein a comparison with the simulation result is also provided, showing a good agreement between the two. It is observed that the output port has a return loss of better than −10 dB from 1.5 GHz to 6 GHz. Figure 6 shows the simulated return loss of input ports when the combiner is working in the even mode of operation (i.e. all the inputs are excited equally with the same phase and amplitude).

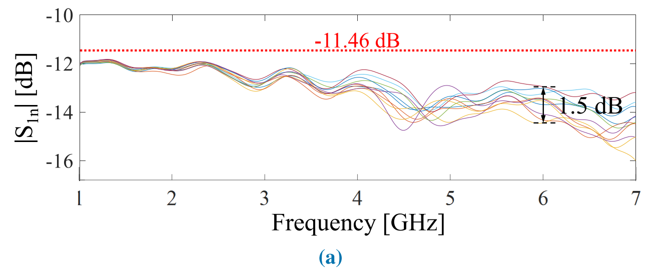

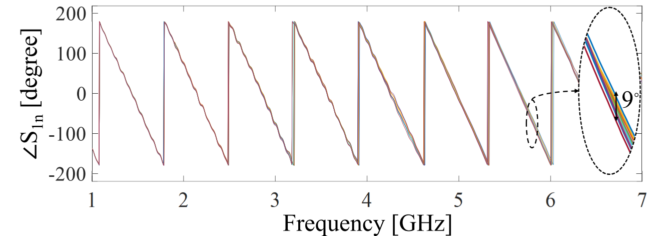

FIGURE 7. The measured (a) magnitude and (b) phase of S_{1n}s, where port 1 is the main (output) port of the combiner.

Figure 7a shows the measured S_{1n} for all the input ports, where port 1 is the main (i.e., output) port. Ideally, for a 14-way power combiner, the transmission loss from each input port to the output port (i.e., $|S_{1n}|$) is −11.46 dB, which is shown as a red dashed line in Figure 7a. However, in this figure, the measured $|S_{1n}|$s show an average loss of between 0.4 dB (at 1.5 GHz) and 2 dB (at 6 GHz) in addition to the ideal transmission loss. This is in good agreement with our full-wave simulation, showing an average loss between 0.25 dB (at 1.5 GHz) and 1 dB (at 6 GHz). Our full-wave simulation showed that at high frequencies the contribution of dielectric loss in the power dissipation within the structure is around 0.6 dB, while that of the metal (copper) loss is 0.4 dB; hence by using dielectric substrates with a lower loss tangent, such as Rogers RT/duroid® 5870 / 5880, one can alleviate the insertion loss at higher frequencies considerably. Moreover, and importantly, in Figure 7a, an amplitude balance of ±0.75 dB (i.e. 1.5 dB) in the worst case (at 6 GHz) is achieved experimentally. Besides that, as seen in Figure 7b, the phase balance of the combiner (i.e., the difference between $\angle S_{n1}$s) was measured to be better than ±4.5 degrees in the entire bandwidth. This is clearer in Figure 8 which shows the worst case of the phase balance between the input ports (at a frequency close to 6 GHz) when one of them (port number 7 where the port numbering can be seen in the inset of Figure 9) was considered as reference and the phase difference of all the other peripheral ports were measured compared to the reference port. The isolation between the input ports obtained using full-wave simulation is shown in Figure 9. It is seen that the minimum isolation which is between two adjacent ports (e.g. port 2 and ports 3 or 15) is 8.6 dB at 6 GHz.

Additional simulations were carried out to analyze the sensitivity of the performance of the design to variations of the parameters which are subjected to more uncertainty in the

TABLE 2. Comparison of the state-of-the-art radial power combiners.

Ref.		FBW [%]	BW [GHz]	No. of Ways	Isolation [dB]	Phase Balance [degree]	Amplitude Balance [dB]	Loss [dB]	Medium	Machine Work Requirement
[19]	Narrowband	10	9.5-10.5	12	Not Reported	±5	±0.5	0.35	Waveguide	Yes
[20]		23.5	9-11.4	9	< −8	±3	±0.25	0.15	Microstrip + Coax	
[10]		25	28-36	20	< −12	±6	±0.45	1	Waveguide	
[21]		25.9	12.1-15.7	8	< −6	Not Reported	±0.6	0.17	Stripline + Cavity	
[22]		27.6	7.8-10.3	8	< −21	±0.75	±0.15	0.2	Coaxial	
[23]	Wideband	71.4	9-19	4	< −4	Not Reported	Not Reported	< 1	Waveguide	
[24]		76.9	0.8-1.8	8	< −5	±2.5	±0.65	< 1.5	Radial Cavity	
This Work		120	1.5-6	14	< −8.6	±4.5	±0.75	< 2	Microstrip	No

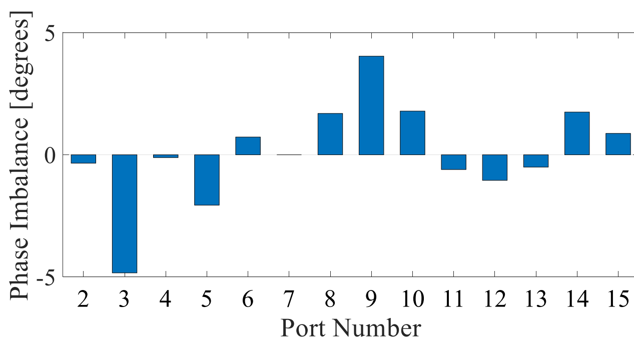

FIGURE 8. The phase differences between the input (split) ports when one of them (port number 7) is taken as reference.

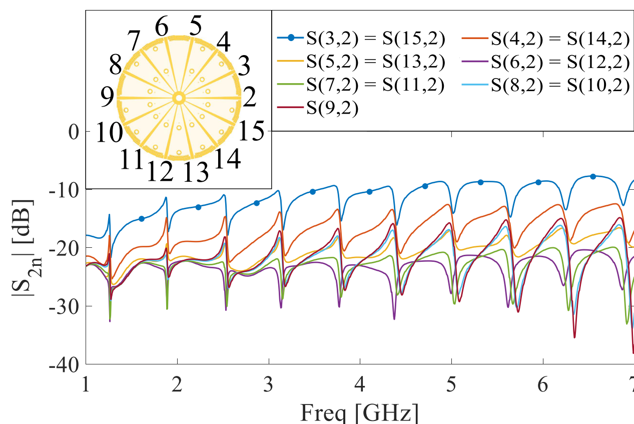

FIGURE 9. Isolation between the input (split) ports.

manufacturing process. In these simulations, the diameter of the central via (D1) was changed by ±0.2 mm. In addition, the gap between the via and ground plane in the middle layer of metallization (see Figure 1b) which has the smallest dimension ((D2-D1)/2) in our design and so is the most sensitive parameter to the PCB manufacturing error was changed by ±50 %. The changes in the output return loss and the phase and amplitude balances were investigated. These results showed that the small variations of D1 and D2 do not have a noticeable effect on the performance of the design; however, the effect on the phase and amplitude balances is slightly more considerable.

Finally, the designed and fabricated radial power combiner is compared with the state-of-the-art radial power combiners in terms of fractional bandwidth (FBW), bandwidth (BW), the number of ways, isolation between the input ports, phase and amplitude balances, loss, transmission medium, and machine work requirement. The comparison results are shown in Table 2 where the rows are sorted in ascending order of FBW. It is evident that with a FBW of 120%, our combiner has a much wider bandwidth than all the other ones, and yet its performance, i.e., its isolation, phase and amplitude balances, and loss is comparable to that of the other works. It should be noted that in Table 2, the loss is somehow proportional to FBW such that the wideband combiners (with a FBW of higher than 70%) exhibit much greater loss than the narrowband ones. In particular, our fabricated combiner, having the widest bandwidth, also has the highest level of loss in the table. Moreover, it should not be forgotten that the microstrip transmission medium which was used in this work intrinsically has a higher loss compared to metallic waveguides, coaxial lines, etc [26]. Most importantly, among all the works presented in Table 2, only our radial power combiner has a fully planar structure (based on microstrip lines) and can be fabricated using a standard PCB technology without requiring any machine work, while all the other works require some kind of machine work.

IV. CONCLUSION

In a conclusion, this paper presented a novel planar 14-way radial power combiner with a two-octave bandwidth. The most distinguishing feature of the proposed combiner is its ease and economy of fabrication using standard PCB manufacturing techniques. Measurement results showed that throughout a 1.5-6 GHz bandwidth, the output port is matched better than −10 dB and the phase and amplitude

balances are better than ±4.5 degrees and ±0.75 dB, respectively. At the highest frequency, the fabricated combiner exhibited an average intersession loss of 2 dB; however, according to our simulation, by using a low-loss dielectric substrate, it can be reduced to around 1 dB.

REFERENCES

[1] K. J. Russell, "Microwave power combining techniques," *IEEE Trans. Microw. Theory Techn.*, vol. MTT-27, no. 5, pp. 472–478, May 1979.

[2] K. Chang and C. Sun, "Millimeter-wave power-combining techniques," *IEEE Trans. Microw. Theory Techn.*, vol. MTT-31, no. 2, pp. 91–107, Feb. 1983.

[3] J. Schellenberg, "The evolution of power combining techniques: From the 60s to today," in *IEEE MTT-S Int. Microw. Symp. Dig.*, May 2015, pp. 1–4.

[4] M. P. DeLisio and R. A. York, "Quasi-optical and spatial power combining," *IEEE Trans. Microw. Theory Techn.*, vol. 50, no. 3, pp. 929–936, Mar. 2002.

[5] A. E. Fathy, S.-W. Lee, and D. Kalokitis, "A simplified design approach for radial power combiners," *IEEE Trans. Microw. Theory Techn.*, vol. 54, no. 1, pp. 247–255, Jan. 2006.

[6] H. Kagan, "N-way power divider (correspondence)," *IRE Trans. Microw. Theory Techn.*, vol. 9, no. 2, pp. 198–199, Mar. 1961.

[7] M. D. Abouzahra and K. C. Gupta, "Multiple-port power divider/combiner circuits using circular microstrip disk configurations," *IEEE Trans. Microw. Theory Techn.*, vol. MTT-35, no. 12, pp. 1296–1302, Dec. 1987.

[8] M. D. Abouzahra and K. C. Gupta, "Analysis and design of five port circular disc structures for six-port analyzers," in *IEEE MTT-S Int. Microw. Symp. Dig.*, Jun. 1985, pp. 449–452.

[9] E. L. Holzman, "An eigenvalue equation analysis of a symmetrical coax line to N-way waveguide power divider," *IEEE Trans. Microw. Theory Techn.*, vol. 42, no. 7, pp. 1162–1166, Jul. 1994.

[10] Q.-X. Chu, D.-Y. Mo, and Q. S. Wu, "An isolated radial power divider via circular waveguide TE_{01} mode transducer," *IEEE Trans. Microw. Theory Techn.*, vol. 63, no. 12, pp. 3988–3996, Dec. 2015.

[11] C. Chang, Z. Xiong, L. Guo, X. Wu, Y. Liu, X. Xing, and Z. Li, "Compact four-way microwave power combiner for high power applications," *J. Appl. Phys.*, vol. 115, Jun. 2014, Art. no. 214502.

[12] R. V. Haro-Báez, J. L. Masa-Campos, J. A. R. Cruz, P. S. Olivares, and E. V. Carrera, "Development of radial Waveguide dividers with large number of ports," in *Proc. Asia–Pacific Conf. Comput. Aided Syst. Eng.*, Jul. 2015, pp. 58–62.

[13] V. Ravindra, H. Saito, J. Hirokawa, and M. Zhang, "Cylindrical cavity microwave power combiner with microstrip line inputs and rectangular waveguide output," in *IEEE MTT-S Int. Microw. Symp. Dig.*, Phoenix, AZ, USA, May 2015, pp. 1–4.

[14] M. Ghanadi, "A new compact broadband radial power combiner," Ph.D. dissertation, Dept. Electrotechnol. Inf., Tech. Univ. Berlin, Berlin, Germany, 2012.

[15] H. Cheng and B. Zhang, "A design of C-band improved radial power combiner," in *Proc. 9th Int. Conf. Solid-State Integr.-Circuit Technol.*, Oct. 2008, pp. 1415–1417.

[16] (2019). *CST-Computer Simulation Technology*. [Online]. Available: http://www.cst.com

[17] L. Guo, J. Li, W. Huang, H. Shao, and T. Ba, "A compact four-way power combiner," *IEEE Microw. Wireless Compon. Lett.*, vol. 27, no. 3, pp. 239–241, Mar. 2017.

[18] L. Guo, J. Li, W. Huang, H. Shao, T. Ba, T. Jiang, Y. Jiang, and G. Deng, "A waveguide magic-T with coplanar arms for high-power solid-state power combining," *IEEE Trans. Microw. Theory Techn.*, vol. 65, no. 8, pp. 2942–2952, Aug. 2017.

[19] R. Kazemi, G. Hegazi, and A. E. Fathy, "X-band all-waveguide radial combiner for high power applications," in *IEEE MTT-S Int. Microw. Symp. Dig.*, May 2015, pp. 1–4.

[20] S. B. Erekson, W. J. D. Johnson, and D. Peroulis, "Design of an airline coax radial power combiner with enhanced isolation," in *IEEE MTT-S Int. Microw. Symp. Dig.*, Jun. 2017, pp. 455–458.

[21] X. Shan and Z. Shen, "A suspended-substrate Ku-band symmetric radial power combiner," *IEEE Microw. Wireless Compon. Lett.*, vol. 21, no. 12, pp. 652–654, Dec. 2011.

[22] L. Guo, J. Li, W. Huang, H. Shao, and T. Ba, "Design of a high-isolation n-way power combiner based on a 2n + 1 port mode network," *IEEE Access*, vol. 6, pp. 6446–6454, 2017.

[23] J.-C. S. Chieh, M. Civerolo, and A. Clawson, "A ultra wideband radial combiner for X/Ku-band using CNC and DMLS processes," *IEEE Microw. Wireless Compon. Lett.*, vol. 25, no. 5, pp. 286–288, May 2015.

[24] Y.-P. Hong, D. F. Kimball, P. M. Asbeck, J.-G. Yook, and L. E. Larson, "Single-ended and differential radial power combiners implemented with a compact broadband probe," *IEEE Trans. Microw. Theory Techn.*, vol. 58, no. 6, pp. 1565–1572, Jun. 2010.

[25] *RO4000 Series High Frequency Circuit Materials*, Rogers Corp., Rogers, CT, USA, 2017.

[26] D. Pozar, *Microwave Engineering*. New York, NY, USA: Wiley, 2011.

SAYYED-HOSSEIN JAVID-HOSSEINI was born in Tehran, Iran. He received the B.Sc. degree in electrical engineering from the K. N. Toosi University of Technology, Tehran, Iran, in 2014, and the M.Sc. degree in satellite engineering from the Iran University of Science and Technology, Tehran, in 2018.

Since 2015, he has been an Antenna and RF-Circuit Designer with ACECR—Nasir Branch, Tehran. His research interests include antennas and microwave circuits both passive and active.

VAHID NAYYERI (S'08–M'14–SM'16) was born in Tehran, Iran. He received the B.Sc. degree from the Iran University of Science and Technology (IUST), Tehran, Iran, in 2006, the M.Sc. degree from the University of Tehran, Tehran, in 2008, and the Ph.D. degree from IUST, in 2013, all in electrical engineering.

From 2007 to 2010, he was an RF-Circuit Designer with the IUST Satellite Research Center. Subsequently, he was the Technical Manager of three research and industrial projects at the Antenna and Microwave Research Laboratory, IUST. In 2012, he joined the University of Waterloo, Waterloo, ON, Canada, as a Visiting Scholar. He is currently an Assistant Professor with the Department of Satellite Engineering, IUST, and also serves as the Co-Director of the Antenna and Microwave Research Laboratory. He has authored and coauthored one book (in Persian) and over 50 journals and conference technical papers. In 2019, he joined the University of Waterloo as a Visiting Professor. His research interests include applied and computational electromagnetics, and microwave circuits.

Dr. Nayyeri was the General Co-Chair of the 1st National Conference on Space Technology and Its Applications, Tehran, in 2019. In 2014, he received the Best Ph.D. Thesis Award from the IEEE Iran Section for his research on the modeling of complex media and boundaries in the finite-difference-time-domain method. He has served as a Reviewer for several journals and conferences.